(*R*/*S*-ClMBA)$_3$GeI$_5$: A Novel Low-Dimensional Ge-Containing Chiral Perovskite

Clarissa Coccia,[a] Massimo Boiocchi,[b] Marco Moroni,[a] Yali Yang,[c] Alessandro Stroppa,[d] and Lorenzo Malavasi,[a,*]

[a]University of Pavia, Department of Chemistry and INSTM, Viale Taramelli 16, 27100, Pavia, Italy
[b]University of Pavia, Centro Grandi Strumenti, Via Bassi 21, 27100, Pavia, Italy
[c]School of Mathematics and Physics, University of Science and Technology Beijing, Beijing 100083, China.
[d]CNR-SPIN c/o Department of Physical and Chemical Sciences, University of L'Aquila, Via Vetoio, I-67100, Coppito, L'Aquila, Italy

ABSTRACT: We report here the first chiral perovskite containing germanium, namely (*R/S*-ClMBA)$_3$GeI$_5$. Single crystal x-ray diffraction shows the formation of a crystal structure composed of GeI$_6$ octahedra arranged in linear zig-zag chains running along the *b*-axis, providing a one-dimensional (1D) system with a novel structural motif. The presence of Ge leads to the highest values of octahedral distortion parameters among chiral perovskites. Chiroptical properties determination by circular dichroism confirms the effective chirality transfer from the ligands to the inorganic framework with asymmetry factors of the order 10^{-3}, with maximum absorbance around 420 nm. The demonstration of the successful preparation of Ge-based chiral perovskites with clear chiroptical properties may open the way for the future design of novel and optimized materials

Chiral perovskites, showing peculiar non-linear optical and spin-dependent properties, are triggering a huge interest for their potential use in different applicative areas such as chiroptoelectronics and spintronics.[1–3] In addition, their intrinsic non-centrosymmetric structure may be exploited in ferroelectric and piezoelectric devices.[4] To date, most of the reported chiral perovskites contain lead, with just one Sn-based composition reported, namely MBA_2SnI_4 (MBA=methylbenzylammonium), and few other examples of Cu-containing phases.[5–7] However, concerns about the toxicity and environmental impact of lead should prompt scientists to explore alternative metals that can offer comparable or even superior performance. This is even more important for a recently developing research field as the one of chiral perovskite. The substitution of lead with alternative elements in perovskite structures presents an opportunity to develop environmentally friendly and sustainable materials while retaining or enhancing their chiral properties. This not only addresses the concerns associated with lead toxicity but also opens up new avenues for exploring novel optoelectronic phenomena and expanding the scope of perovskite-based devices.

Indeed, the number of lead-free chiral perovskite, as mentioned, is extremely limited and to understand the fundamental mechanisms underlying the chirality in perovskite materials, unveil the role of central metal atom, and devise novel and advanced materials, is crucial to explore the synthesis and characterization of novel lead-free chiral perovskites.

Herein we report the first iodide Ge-based chiral perovskite synthesized by using the ClMBA (ClMBA=4-chloro-methylbenzylamine) chiral ligand in the *R*-/*S*- enantiopure isomers. Specifically, we afforded the synthesis and characterization of the low-dimensional, 1D, $(Cl\text{-}MBA)_3GeI_5$ material.

Light orange single crystals of $(R\text{-}ClMBA)_3GeI_5$ and $(S\text{-}ClMBA)_3GeI_5$ have been grown as described in the Supporting Information (SI) and subjected to single-crystal X-ray diffraction (SCXRD). A sketch of the two structures is reported in Figure 1 together with a picture of the $(R\text{-}ClMBA)_3GeI_5$ single crystals, while Table 1 reports selected crystallographic data. The structural

stability of the samples has been checked by differential scanning calorimetry (DSC) in the temperature range -80-130°C showing no evidence of any phase transitions (see Figure S1).

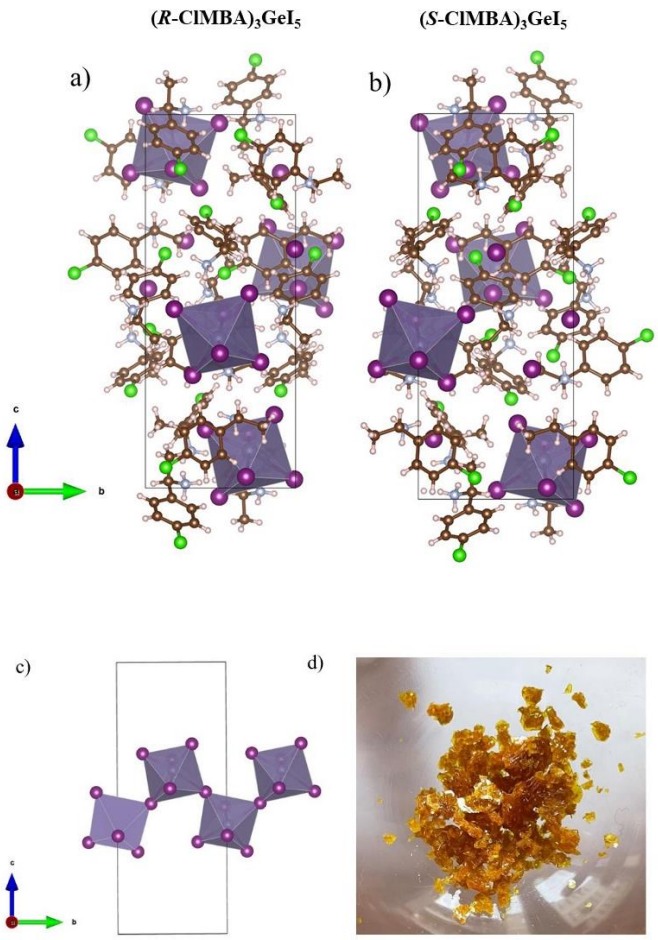

Figure 1. a) and b) represent sketches of the crystal structures of (*R*-ClMBA)$_3$GeI$_5$ and (*S*-ClMBA)$_3$GeI$_5$, respectively; c) detail of the zig-zag linear chain arrangement along the *b*-axis; d) appearance of the single crystals of (*R*-ClMBA)$_3$GeI$_5$.

Table 1. Crystallographic data for (*R*-Cl-MBA)$_3$GeI$_5$ and (*S*-Cl-MBA)$_3$GeI$_5$.

	(*R*-ClMBA)$_3$GeI$_5$	**(*R*-ClMBA)$_3$GeI$_5$**
Formula weight	2353.98	2353.98
Temperature	298	298
Wavelength	0.7107	0.7107
Crystal system	Monoclinic	Monoclinic
Space group	$P2_1$	$P2_1$
Lattice parameters	a = 18.7304(5)	a = 18.7271(6)
	b = 8.8918(2)	b = 8.8982(2)
	c = 23.0151(8)	c = 23.0211(8)
	β= 105.998(3)	β = 105.967(3)
Lattice Volume	3684.64(19)	3688.2(2)
Z	2	2
CCDC code	2283932	2283931

As can be appreciated from Table 1, the two chiral samples of (*R*-ClMBA)$_3$GeI$_5$ and (*S*-ClMBA)$_3$GeI$_5$ crystallize in the non-centrosymmetric $P2_1$ space group (n° 4), one of the 65 Sohncke space groups, and form two inverted crystal structures. The crystal structure is composed of GeI$_6$ octahedra arranged in linear zig-zag chains running along the *b*-axis (cfr. Fig 1c) with Ge-I-Ge bond angle in the range 155.93-157.70°, leading to a one-dimensional (1D) perovskite. The octahedra are distorted presenting six different Ge-I bond-lengths grouped in two sets of similar values, *i.e.* around 2.8 and 3.3 Å. A full list of octahedra parameters is reported in Table S1 of the SI. To the best of our knowledge, the only other example of such structural arrangement has been reported for a guanidinium containing lead iodide perovskite, namely (C(NH$_2$)$_3$)$_3$PbI$_5$.[8] Concerning chiral perovskites, few 1D systems have been recently reported by including the *R*/*S*-2-aminomethylpyrrolidine (AMP) cation in lead bromide compositions (*R*/*S*-AMP)$_2$Pb$_3$Br$_{10}$), and N-

ethyl-quinuclidine (EQ) in a lead iodide perovskite ($EQPbI_3$).[9,10] Finally, the only other lead-free 1D perovskite, namely [(*R/S*)-β-MPA]$_4AgBiI_8$ (MPA= methylphenethylammonium), has been reported in 2021 by Liu and co-workers.[11] Another interesting feature of the present Ge-based chiral perovskite is related to the octahedral distortion parameters which can be quantified in terms of bond length distortion index (*D*) and bond angle variance (σ^2).[12,13] The larger the value of *D* and σ^2, the larger becomes the octahedral distortion. The *D* parameter for (*R*-ClMBA)$_3GeI_5$ and (*S*-ClMBA)$_3GeI_5$ is in the range 0.071-0.075 with bond angle variance in the range 12.59-15.70 deg^2, respectively. Such distortion level surpasses the actual highest value of octahedral distortion in chiral perovskites which has been previously reported for (*R*-/*S*-MBA)$_2SnI_4$ having a similar *D* parameter and σ^2 of about 10.3 deg^2.[5] We can correlate this high level of distortion to the presence of Ge cation. As a matter of fact, we already observed an increased level of octahedral deformation by moving from Pb to Sn and to Ge in related low-dimensional perovskites.[14,15]

To sum up, the (*R*-ClMBA)$_3GeI_5$ and (*S*-ClMBA)$_3GeI_5$ 1D chiral perovskites represent not only the first examples of Ge-containing materials but the structural investigation allowed to highlight an unusual and uncommon octahedra connection network leading also to the highest level of octahedral distortion reported so far in chiral perovskites.

First-principles calculations are performed to further investigate the structure and electronic properties of (*R*-ClMBA)$_3GeI_5$ and (*S*-ClMBA)$_3GeI_5$. The atomic positions of the structures are optimized with the lattice parameters being fixed to the experimental values. After optimization and taking (*R*-ClMBA)$_3GeI_5$ as example, the GeI_6 octahedra shows 14° tilting angle about the axis vertical to the inorganic GeI_5 layers, as shown in Figure 2a. Such tilting angle leads to the Ge-I-Ge bond angle of about 152.04° which is very close to the experimental angle 157.70°. For the other two axes of the pseudo cubic of GeI_6, which lie in the GeI5 layers, there are no obvious tilting. The Ge-I bond lengths are also shown in Figure 2a. The band structure of (*R*-ClMBA)$_3GeI_5$ is shown in Figure 2b in which an indirect band gap of about 2.65 eV is presented with the VBM at Γ(0 0 0) point and CBM at A(-0.5 0 0.5) point. We note that the calculated band gap value is in well agreement with the experimental

one, *i.e.*, 2.69 eV (see later in the text). Furthermore, the band structure with considering the spin-orbital coupling (SOC) is also calculated (not shown here), however it shows very little difference with the band structure without SOC. In Figure 2c, we show the projected density of states of (*R*-ClMBA)$_3$GeI$_5$. One can easily find that the VBM is mainly contributed by the I atoms from the GeI$_5$ inorganic framework, while the CBM is mainly contributed by the C atoms of the organic molecules.

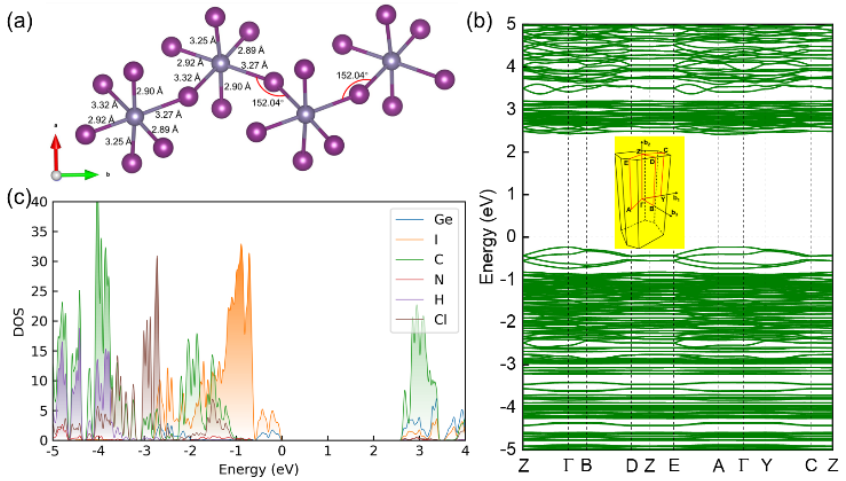

Figure 2. Structure and electronic properties of (*R*-ClMBA)$_3$GeI$_5$. (a) Structure information of relaxed (*R*-ClMBA)$_3$GeI$_5$. (b) Band structure of (*R*-ClMBA)$_3$GeI$_5$. (c) Projected density of states of (*R*-ClMBA)$_3$GeI$_5$.

Optical properties have been measured by UV-Vis (on powdered single crystals) and CD spectroscopy (on dip-coated polycrystalline thin films of about 400 nm thickness) of (*R*-ClMBA)$_3$GeI$_5$ and (*S*-ClMBA)$_3$GeI$_5$. Details about thin films preparation are reported in the SI. Room temperature steady-state photoluminescence measurements were attempted but not clear emission was observed for the two samples.

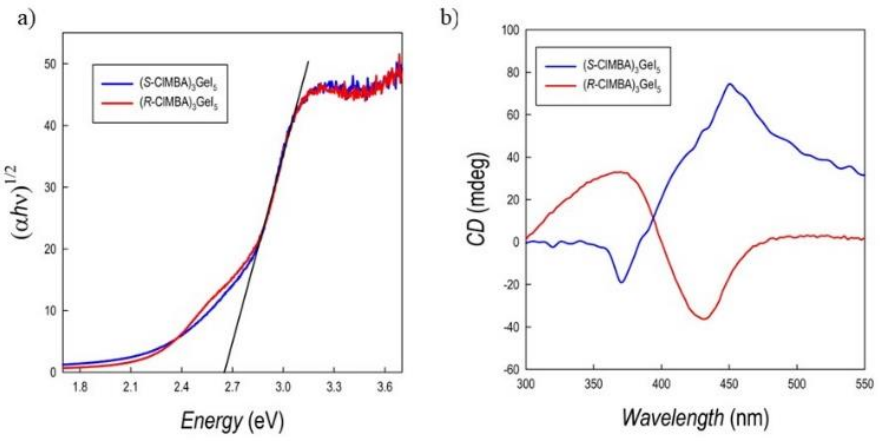

Figure 3. a) Tauc plot and b) CD spectra for (*R*-ClMBA)$_3$GeI$_5$ and (*S*-ClMBA)$_3$GeI$_5$.

Linear absorption spectra (see Figure S2) show quite sharp edge around 420 nm without any indication of excitonic peak in agreement with the results on (*R*-MBA)$_2$SnI$_4$ and (*S*-MBA)$_2$SnI$_4$ where such behavior was correlated with the high level of structural distortion which is even greater for the present samples.[5] The band-gap values extrapolated from the Tauc plots (Figure 3a) for indirect transitions are 2.69 and 2.71 eV, respectively, for (*R*-ClMBA)$_3$GeI$_5$ and (*S*-ClMBA)$_3$GeI$_5$. The CD spectra present two peaks in the range 350-460 nm, namely one centered around 371 nm and the second one around 440 nm in good agreement with the absorption edge. The presence of opposite sign CD peaks for the two samples confirm the chirality transfer from the chiral ligand ClMBA to the inorganic framework. As a matter of fact, the two chiral amines have CD spectra with a peak centered around 245 nm (see Figure S3). The chiral anisotropy factor, g_{CD}, has been calculated from the CD measurements and resulted to be around 4×10^{-3}. It is not possible, at present, to make a direct comparison of the chiroptical properties of (*R*-ClMBA)$_3$GeI$_5$ and (*S*-ClMBA)$_3$GeI$_5$ with available data on chiral perovskites due to the fact that this is the first composition containing germanium but, more importantly, the structural motif of the present samples has not been found in any other chiral perovskite to date. However, we can report the value of the g_{CD} for the two 1D perovskites of this work are in line with the values found in 2D perovskites, specifically containing tin, with lead-based materials showing, in general slightly lower values of the order of $\times 10^{-4}$.[16]

To conclude, this paper reports the first Ge-containing chiral perovskites to date including the (*R*-/*S*-)ClMBA chiral amines. The prepared pair of chiral samples, namely (*R*-ClMBA)$_3$GeI$_5$ and (*S*-ClMBA)$_3$GeI$_5$, show a peculiar structural motif characterized by a zig-zag linear arrangement of corner-sharing GeI$_6$ octahedra. Chiroptical measurements confirm an effective chirality transfer from the chiral ligand to the inorganic framework. The demonstration of the successful preparation of novel compositions, specifically lead-free, in the field of chiral perovskite is of pivotal importance for its further development. Significant efforts are still needed to unveil solid structure-property correlations which can help the engineering of materials with tailored chiroptical features. On this line, the synthesis of rational series of compositions with analogous crystal structure and chiral amines and different central metals are needed to unveil the role, among others, of structural distortions and spin-orbit coupling effects on the chiroptical properties. Further investigations about the role of electric polarization are in progress.

Acknowledgements

LM acknowledges support from the Ministero dell'Università e della Ricerca (MUR) and the University of Pavia through the program "Dipartimenti di Eccellenza 2023–2027." We acknowledge the CINECA award under the ISCRA initiative, for the availability of high performance computing resources and support. A.S. would like to acknowledge Kaidi Xu (Southest University – China) for useful discussions during his visiting stay at CNR-SPIN (L'Aquila) in May-July 2023.

Associated Content

Experimental section, Table S1, Figures S1-S3 reporting the thermal analysis of the samples, the UV-Vis spectra, and the CD spectra of the chiral amines. A.S. would like to acknowledge Kaidi Xu (Southest University – China) for useful discussions during his visiting stay at CNR-SPIN (L'Aquila) in May-July 2023.

REFERENCES

(1) Dang, Y.; Liu, X.; Cao, B.; Tao, X. Chiral Halide Perovskite Crystals for Optoelectronic Applications. *Matter* **2021**, *4* (3), 794–820. https://doi.org/10.1016/j.matt.2020.12.018.

(2) Dong, Y.; Zhang, Y.; Li, X.; Feng, Y.; Zhang, H.; Xu, J. Chiral Perovskites: Promising Materials toward Next-Generation Optoelectronics. *Small* **2019**, *15* (39), 1902237. https://doi.org/10.1002/smll.201902237.

(3) Long, G.; Sabatini, R.; Saidaminov, M. I.; Lakhwani, G.; Rasmita, A.; Liu, X.; Sargent, E. H.; Gao, W. Chiral-Perovskite Optoelectronics. *Nat Rev Mater* **2020**, *5* (6), 423–439. https://doi.org/10.1038/s41578-020-0181-5.

(4) Ma, J.; Wang, H.; Li, D. Recent Progress of Chiral Perovskites: Materials, Synthesis, and Properties. *Adv. Mater.* **2021**, *33* (26), 2008785. https://doi.org/10.1002/adma.202008785.

(5) Lu, H.; Xiao, C.; Song, R.; Li, T.; Maughan, A. E.; Levin, A.; Brunecky, R.; Berry, J. J.; Mitzi, D. B.; Blum, V.; Beard, M. C. Highly Distorted Chiral Two-Dimensional Tin Iodide Perovskites for Spin Polarized Charge Transport. *J. Am. Chem. Soc.* **2020**, *142* (30), 13030–13040. https://doi.org/10.1021/jacs.0c03899.

(6) Hao, J.; Lu, H.; Mao, L.; Chen, X.; Beard, M. C.; Blackburn, J. L. Direct Detection of Circularly Polarized Light Using Chiral Copper Chloride–Carbon Nanotube Heterostructures. *ACS Nano* **2021**, *15* (4), 7608–7617. https://doi.org/10.1021/acsnano.1c01134.

(7) Lu, Y.; Wang, Q.; He, R.; Zhou, F.; Yang, X.; Wang, D.; Cao, H.; He, W.; Pan, F.; Yang, Z.; Song, C. Highly Efficient Spin-Filtering Transport in Chiral Hybrid Copper Halides. *Angew. Chem. Int. Ed.* **2021**, *60* (44), 23578–23583. https://doi.org/10.1002/anie.202109595.

(8) Wilke, M.; Casati, N. Insight into the Mechanochemical Synthesis and Structural Evolution of Hybrid Organic-Inorganic Guanidinium Lead(II) Iodides. *Chem. Eur. J.* **2018**, *24* (67), 17701–17711. https://doi.org/10.1002/chem.201804066.

(9) Liu, H.-L.; Ru, H.-Y.; Sun, M.-E.; Wang, Z.-Y.; Zang, S.-Q. Mixed-Cation Chiral Perovskites Displaying Warm-White Circularly Polarized Luminescence. *Sci. China Chem.* **2023**, *66* (5), 1425–1434. https://doi.org/10.1007/s11426-022-1531-9.

(10) Fu, D.; Hou, Z.; He, Y.; Liu, J.-C.; Lv, H.-P.; Tang, Y.-Y. Multiaxial Ferroelectricity and Ferroelasticity in a Chiral Perovskite. *Chem. Mater.* **2022**, *34* (7), 3518–3524. https://doi.org/10.1021/acs.chemmater.2c00546.

(11) Li, D.; Liu, X.; Wu, W.; Peng, Y.; Zhao, S.; Li, L.; Hong, M.; Luo, J. Chiral Lead-Free Hybrid Perovskites for Self-Powered Circularly Polarized Light Detection. *Angew. Chem. Int. Ed.* **2021**, *60* (15), 8415–8418. https://doi.org/10.1002/anie.202013947.

(12) Baur, W. H. The Geometry of Polyhedral Distortions. Predictive Relationships for the Phosphate Group. *Acta Crystallogr B Struct Sci* **1974**, *30* (5), 1195–1215. https://doi.org/10.1107/S0567740874004560.

(13) Robinson, K.; Gibbs, G. V.; Ribbe, P. H. Quadratic Elongation: A Quantitative Measure of Distortion in Coordination Polyhedra. *Science* **1971**, *172* (3983), 567–570. https://doi.org/10.1126/science.172.3983.567.

(14) Chiara, R.; Accorsi, G.; Listorti, A.; Coduri, M.; Coccia, C.; Tedesco, C.; Morana, M.; Malavasi, L. Halide Alloying and Role of Central Atom on the Structural and Optical Properties of Decylammonium Germanium 2D Perovskites. *APL Energy* **2023**, *1* (1), 016101. https://doi.org/10.1063/5.0146748.

(15) Chiara, R.; Morana, M.; Boiocchi, M.; Coduri, M.; Striccoli, M.; Fracassi, F.; Listorti, A.; Mahata, A.; Quadrelli, P.; Gaboardi, M.; Milanese, C.; Bindi, L.; De Angelis, F.; Malavasi, L. Role of Spacer Cations and Structural Distortion in Two-Dimensional Germanium Halide Perovskites. *J. Mater. Chem. C* **2021**, *9* (31), 9899–9906. https://doi.org/10.1039/D1TC02394B.

(16) Malavasi, L.; Moroni, M.; Coccia, C. *Chiral Metal Halide Perovskites: Focus on Lead-Free Materials and Structure-Property Correlations*; preprint; Chemistry and Materials Science, 2023. https://doi.org/10.20944/preprints202307.0836.v1.